The sensitivity of Global Climate Model simulations to the representation of soil moisture heterogeneity

Hadley Centre technical note 41

N. Gedney and P. M.Cox

23 December 2002

Met Office

The sensitivity of Global Climate Model simulations to the representation of soil moisture heterogeneity

N. Gedney and P. M. Cox

Hadley Centre, Met Office, Bracknell, Berks RG12 2SY, UK

December 23, 2002

Abstract

Improving the treatment of sub-gridscale soil moisture variations is recognised as a priority for the next generation of Land Surface Schemes (IPCC (2001)). Here we assess the impact of an improved representation of sub-gridscale soil moisture heterogeneity on Global Climate Model (GCM) simulations of current and future climates, carried out using the HadAM3 GCM coupled to the MOSES land-surface scheme (Cox *et al* (1999)). MOSES was adapted to make use of TOPMODEL algorithms (Beven and Kirkby (1979)) which relate the local water table depth to the gridbox mean water table depth, assuming that sub-gridscale topography is the primary cause of soil moisture heterogeneity. This approach was also applied to produce a novel model for wetland area, which can ultimately be used to interactively model methane emissions from wetlands. The modified scheme was validated off-line by forcing with near-surface GSWP data (Dirmeyer *et al* (1999)), and online within the HadAM3 global climate model (GCM). In both cases it was found to improve the present-day simulation of runoff and produce realistic distributions of global wetland area. (Precipitation was also improved in the online simulation). The new scheme results in substantial differences in the modelled sensitivity of runoff to climate change, with implications for the modelling of hydrological impacts.

1 Introduction

The historical development of GCM land surface schemes (LSSs) has tended to focus on the vertical transfer of water (and heat) through the soil and canopy. The evaporative fluxes from the bare soil and the wet and dry parts of the canopy are generally modelled separately, and vertical transfers of water and moisture in the soil are explicitly modelled using multi-layer models. The Met Office Surface Exchange Scheme, MOSES (Cox *et al* (1999)), has a typical structure for this generation of LSSs, using 4 soil layers in the vertical with depths chosen to capture important soil temperature cycles (for MOSES the default thicknesses from the surface downwards are 0.1m, 0.25m, 0.65m, 2.0m). Recognising the strong non-linearity of the Richards' equation, some GCM land-surface modellers have recently increased the vertical resolution of their soil models (de Rosnay *et al* (2002)) to further improve the accuracy with which vertical flows can be captured.

This continuing improvement in the representation of vertical processes is in stark contrast to progress on the representation of horizontal heterogeneity, such that the latter is now seen as a priority for the next generation of LSSs (Polcher *et al* (2002)). Current LSSs are applied directly at the GCM resolution, which is much too coarse to explicitly represent important aspects of land-surface heterogeneity. Surface fluxes tend to be calculated from the gridbox mean soil water stores, without taking account of sub-grid variations in soil moisture which can significantly modify gridbox mean fluxes (and therefore the GCM climate).

In reality, even within a single catchment there can be large variations of soil moisture due to a number of factors, including soil properties and topography. Overland flow usually occurs either when the rainfall rate exceeds the soil saturated hydraulic conductivity (Hortonian runoff) or when the soil surface becomes saturated from beneath (Dunne runoff). If this soil moisture variability is not modelled then localised saturated areas are not represented and an underestimate of surface runoff is likely to occur. Such omissions may affect the accuracy of the simulated hydrological partitioning within the climate model.

In common with other GCM LSSs, MOSES (Cox *et al* (1999)) has a relatively detailed depiction of the gridbox mean fluxes, but no sub-gridscale horizontal soil moisture variability. To address this

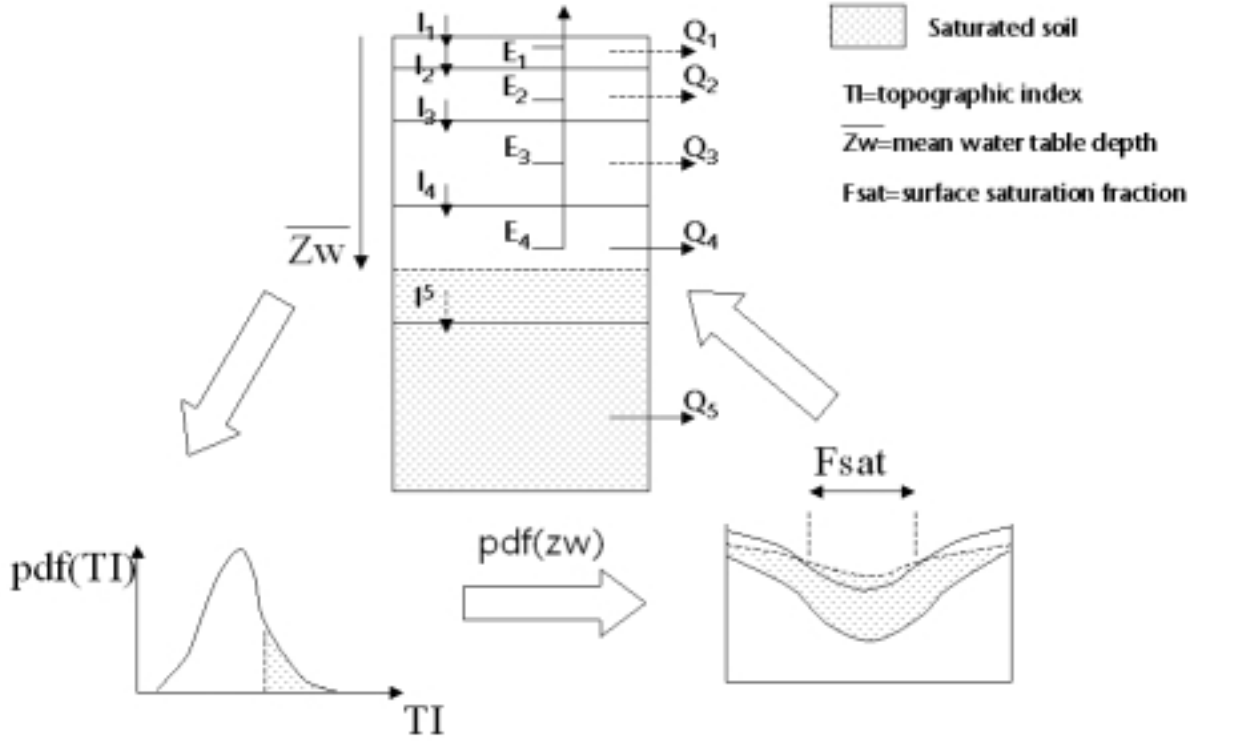

Figure 1:
Schematic diagram of the combined MOSES-TOPMODEL approach.

limitation we have coupled a reduced form of TOPMODEL (Beven (1986) and Beven and Kirkby (1979)) to MOSES. TOPMODEL is based on the hypothesis that topography is the primary cause of water table variability within many catchments. In order to apply the TOPMODEL idea, we have assumed that similar relationships apply to each GCM gridbox. For simplicity we ignore sub-gridscale variations in soil parameters at this stage, although a simple extension of TOPMODEL has been developed to deal with some aspects of soil heterogeneity (Sivapalan *et al* (1987)).

2 Overview of Model

In order to parameterise ground water flow Q, a deep water store (thickness 12 metres) is added beneath the 4 layer soil model of MOSES. The gridbox mean water table depth $\overline{z_w}$ is modelled *prognostically* within this deep store:

$$\rho\theta_{sat}\frac{d\overline{z_w}}{dt} = I_5 - Q_5 \tag{1}$$

where ρ is the density of water and θ_{sat} is the saturated volumetric water content. I_i and Q_i are the infiltration into and base flow out of the ith layer respectively (see Fig 1). If this layer saturates, the water table depth is then *diagnosed* to be within the deepest soil layer which is not saturated. In addition to the vertical drainage fluxes between soil layers, base flow Q_i occurs out of any layer which is below or contains the top of the water table:

$$\Delta z_i \rho \frac{d\theta_i}{dt} = I_i - E_i - Q_i \tag{2}$$

where Δz_i is the thickness of the soil layer, θ_i volumetric fraction water content and E_i is the extraction due to evaporation out the ith soil layer. The partitioning of the base flow out of a layer is based on the relative amount of water table within that layer.

Having calculated the gridbox mean water table depth, an estimate of its spatial variability is required to predict the extent of saturation at the surface, and hence the amount of Dunne runoff. The basic theory from which this is derived is described in detail in Sivapalan *et al* (1987). A brief overview is given below.

a Overview of TOPMODEL

If the water table within a catchment is assumed to be in steady state, then a general solution for the local water table depth z_{wl} relative to the mean may be obtained if the saturated conductivity K_{sat} decreases exponentially with depth as follows:

$$K_{sat}(z) = K_{sat}(0) \exp(-fz) \tag{3}$$

where $K_{sat}(0)$ is the saturated conductivity at the surface and f is an exponent describing the reduction of saturated conductivity with depth. (Beven (1982) cite many examples where this is a reasonable assumption).

The local downslope flow, q_l, at any point is given by:

$$q_l = T(z_{wl}) \tan \beta_l \tag{4}$$

where β_l is the local topographic gradient, and the local transmissivity $T(z_{wl})$ is given by integrating equation 3 vertically through the saturated zone, from the local water table depth, z_{wl}, to the bottom of the profile ,Z_{wmax}:

$$T(z_{wl}) = \int_{Zwl}^{Zwmax} K_{sat}(z) dz \tag{5}$$

TOPMODEL assumes a quasi-equilibrium state in which the local downslope flow, q_l, is balanced by recharge from a local upslope area, a_l. Integrating over the catchment yields a relationship between the local water table depth, z_{wl}, and the gridbox mean water table depth, $\overline{z_w}$:

$$f\{z_{wl} - \overline{z_w}\} = \Lambda_l - \overline{\Lambda} \tag{6}$$

where Λ_l is the local "topographic index" given by:

$$\Lambda_l = \ln\left(\frac{a_l}{\tan \beta_l}\right) \tag{7}$$

and $\overline{\Lambda}$ is the area-average of Λ_l over the catchment area. Equation 6 is especially valuable because it relates the local moisture status (as given by z_{wl}) to the catchment mean moisture status (as represented by $\overline{z_w}$) based purely on the sub-gridscale variations in topography. Larger than average values of Λ_l are indicative of areas with a higher than average water table (e.g. valley bottoms), while lower than average Λ_l is representative of a deeper than average water table (e.g. at hilltops).

Most importantly for our application, this equation can be integrated to yield the fraction of the gridbox which is saturated at the surface (i.e. a water-table at or above the surface), and which will therefore generate saturation excess (or "Dunne") runoff.

Furthermore, an equation for the catchment averaged base flow per unit area, Q, can be derived by combining equations 7 and 4 and integrating:

$$Q = T(\overline{z_w}) \exp(-\overline{\Lambda}) \tag{8}$$

b Extension of TOPMODEL

We have extended the Sivapalan *et al* (1987) formulation to cover any generalised function of K_{sat} with depth, relaxing the assumption that K_{sat} varies exponentially throughout the profile. Instead we only assume that exponential decay occurs within the saturated zone beneath the 4 layer soil model of MOSES. In principle this allows observed soil parameter profiles to be used in the top 3 metres of the profile, although for simplicity we have assumed uniform K_{sat} in the sensitivity studies presented here. Beneath the MOSES soil model K_{sat} decays in the standard TOPMODEL manner, as given by equation 3, with a value of $f = 0.5$ which was chosen to minimise the errors in off-line global mean runoff simulation.

To make further progress we assume that the mean water table depth corresponds approximately to the mean topographic index. Since q_l/a_l is assumed to be constant, the local water table depth z_{wl} is related to the local topographic index by:

$$\ln\left[\frac{T(z_{wl})}{T(\overline{z_w})}\right] = \Lambda_l - \overline{\Lambda} \tag{9}$$

We have used a global topographic index dataset a (Verdin and Greenlee (1996)) to produce a statistical distribution of this field within each climate model gridbox. This dataset is at a 1km x 1km resolution which is too low to be strictly valid for the TOPMODEL concept, as it cannot resolve hills and valleys. However topography tends to exhibit self-similarity (Brown and Scholz (1985)) so we use this as a first approximation until a more detailed dataset is available at the global scale.
From equation 9 the local water table is at or above the surface when the local topographic index is greater than a critical value Λ_{cr}^{min} (see Figure 1) which is defined as:

$$\Lambda_{cr}^{min} = \ln\left[\frac{T(0)}{T(\overline{z_w})}\right] + \overline{\Lambda} \tag{10}$$

The fraction of the surface that is saturated F_s is then given by the relative area where $\Lambda_l \geq \Lambda_{cr}^{min}$ over the whole gridbox (see Figure 1). Under partially saturated conditions the gridbox mean net infiltration I_1 into the top soil layer is therefore reduced by:

$$I_1 = (1 - F_s) I_{H1} \tag{11}$$

where I_{H1} is the infiltration rate into the soil if only Hortonian runoff is considered.

In addition to the surface saturation fraction, we also require an estimate of actual wetland extent, as this can be validated against observations and can be used in the interactive modelling of methane emissions from wetlands. Wetland is limited to areas of stagnant water. However, if the water table rises well above the surface, this can be viewed as indicative of stream flow. We therefore define a maximum critical topographic index parameter Λ_{cr}^{max} to calibrate the wetland area with observations. It is assumed that where the local topographic index is greater than the critical value ($\Lambda_l > \Lambda_{cr}^{max}$) the water table is too deep and results in significant flow. Hence a local point is assumed to be wetland only when:

$$\Lambda_{cr}^{max} \geq \Lambda \geq \Lambda_{cr}^{min} \tag{12}$$

where the global parameter Λ_{cr}^{max} is chosen to give the best agreement with observations.

However under partially frozen conditions one would not expect significant flow velocity. In order to account for this, the extent of soil freezing at the mean water table depth is used to calculate an effective wetland fraction:

$$F_{wet}^{eff} = \frac{\theta_u}{\theta_u + \theta_f} F_{wet} + \frac{\theta_f}{\theta_u + \theta_f} F_{sat} \tag{13}$$

where θ_u θ_f are the frozen and unfrozen soil moisture fractions respectively at the mean water table depth.

3 Experiments

We assess the standard version of the MOSES land surface scheme (CTL) against MOSES modified to include the TOPMODEL-based large-scale hydrology parameterisation (LSH), both off-line and online within the climate model. Off-line studies have the advantage of using realistic near-surface forcing data, thereby allowing a direct assessment of the LSS performance against observations. Data from the Global Soil Wetness Project (GSWP) (Dirmeyer *et al* (1999)) for years 1987 and 1988 is used for this purpose. The GSWP data is a combination of observations and analyses at the 6 hourly timescale. Each LSS is spun up by repeatedly forcing it with the 1987 data until equilibrium is reached. The models are then run from the spun up state for two more years with the 1987 and then the 1988 forcing data. The output from the final two years is compared with observations.

The online study is carried out with the host Met Office GCM HadAM3 (Pope *et al* (2000)). The sea surface temperature and sea-ice fields are both prescribed from climatological monthly means.

4 Results

a Off-line validation

Fig 2a compares the control off-line run using the standard MOSES LSS (CTL) with the observed ratio of annual mean runoff (Fekete *et al* (2000)) to precipitation (Xie and Arkin (1997)). (We use this ratio so that when analysing the GCM simulations we can reduce the influence of the error in the GCM simulation of precipitation on that of the runoff).

Fig 2a shows the percentage error in the control CTL run. In a majority of regions, there is a systematic underestimation of runoff. This is to be expected, given the lack of soil moisture heterogeneity in the LSS. Fig 2b gives the absolute change in percentage errors between the CTL and LSH simulations. (Green and blue signify an improvement of the LSH simulation over the CTL, and orange and red a degradation in performance). Over most regions the LSH scheme increases runoff and therefore produces an improvement. Table 1 shows the resulting reduction in the annually averaged, land mean biases and root mean square (RMS) errors. The overall reduction in bias is from about 37% to 25% and RMS is improved by roughly 5%.

Table 2 gives a breakdown of the modelled annual mean flow for the largest basins and compares them to the UNESCO (1971) observations. You can again see the tendency for the standard MOSES

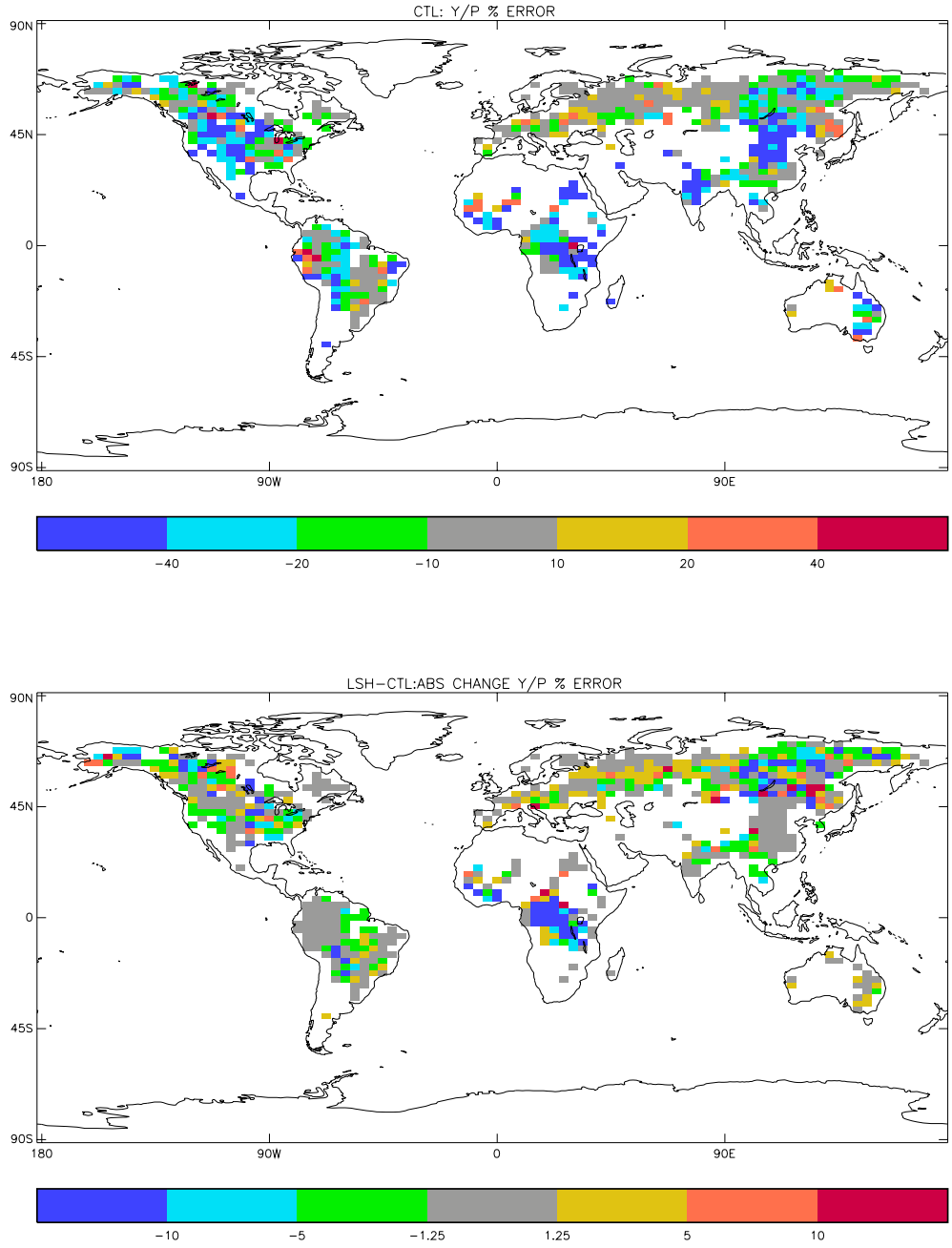

Figure 2:

The impact of including the new large-scale hydrology (LSH) parameterisation on the off-line simulation of the ratio of annual mean runoff to annual mean precipitation Y/P. (The precipitation and runoff observed datasets used are Xie and Arkin (1997) and GRDC Fekete *et al* (2000) respectively. The blank areas in the Figure correspond to where there is no runoff data). a) Percentage error in Y/P for the standard MOSES simulation (CTL). (Green/blue colours signify an underestimate and orange/red an overestimate). b) Absolute change in percentage error in Y/P within the LSH simulation. (Green/blue colours signify an improvement, orange/red signify a deterioration).

	Y/P	RMS error Y/P
OBS	0.380	—
CTL	0.239	0.207
LSH	0.284	0.197

Table 1:

Off-line simulations of annually averaged, land mean runoff/precipitation ratio and the RMS errors.

River Basin	OBS Flow	CTRL Flow	CTRL-OBS	LSH1.1-OBS
	mm/day	mm/day	mm/day	mm/day
AMAZON	2.89	1.95	-0.94	-0.94
ZAIRE*	1.00	0.30	-0.70	-0.22
MISSISSIPPI*	0.46	0.22	-0.24	-0.19
OB	0.37	0.44	0.07	0.11
YENISEI*	0.63	0.59	-0.04	0.00
LENA*	0.58	0.42	-0.16	-0.11
PARANA	0.74	0.94	0.20	0.27
NILE	0.13	0.15	0.02	0.20
AMUR*	0.48	0.31	-0.17	-0.09
CHANG-YIANG	1.46	1.57	0.11	0.12
GANGES+B.*	1.83	0.78	-1.05	-1.00
MACKENZIE*	0.50	0.28	-0.22	-0.17
VOLGA*	0.51	0.42	-0.09	-0.05
NELSON*	0.21	0.12	-0.09	0.04
HUANG HO*	0.13	0.03	-0.10	-0.09
MURRAY	0.02	0.02	0.00	0.00
ORANGE	0.02	0.06	0.04	0.06
ORINOCO*	3.20	1.69	-1.51	-1.49
INDUS	0.41	0.28	-0.14	-0.14
DANUBE	0.69	1.00	0.31	0.45
YUKON*	0.70	0.33	-0.37	-0.30
MEKONG*	1.90	0.43	-1.47	-1.31
COLUMBIA	0.76	0.17	-0.59	-0.59
SAO FRANCISCO*	0.40	0.56	0.16	0.06
KOLYMA*	0.53	0.37	-0.16	-0.10
NIGER*	1.08	0.87	-0.21	0.04
ALL BASINS*	0.96	0.65	-0.31	-0.22

Table 2:

Off-line simulation annual mean (1987-1988), basin averaged runoff compared to UNESCO (1971) Observations. (Those basins with an improved simulation with LSH have a * subscript).

	Y/P	RMS error Y/P	P	RMS error P	Y	RMS error Y
OBS	0.380	—	1.92	—	0.96	—
CTL	0.319	0.214	2.37	0.68	1.10	0.74
LSH	0.337	0.212	2.32	0.65	1.11	0.73

Table 3:
Online simulation of annually averaged, land mean hydrological fields and the RMS errors.

model to underestimate runoff. This tendency is generally reduced with the LSH model, overall by about a third with this dataset. Out of the twenty six basins assessed, sixteen show an improvement, and only six are worse.

We have also assessed the off-line modelled natural wetland fraction, where this is defined as the total wetland fraction over the non-agricultural fraction of the gridbox only. There is generally a good correspondence between the model (Fig 3a) and the Aselmann and Crutzen (1989) observed dataset of natural wetland fraction (Fig 3c), but the model tends to underestimate the magnitude at high latitudes. This could be because we currently neglect the effect of the near-surface, high soil carbon content in high latitude peat lands on the porosity, and therefore on the hydraulic conductivity variation with depth.

b Online validation

We now assess the hydrological budget online within the GCM to see how the two LSSs behave in the climate model. Fig 4 shows the land averaged, zonal means of precipitation, total runoff and surface runoff under the simulated present day climate. HadAM3 has a tendency to be overestimate precipitation (Fig 4a). However this error is consistently reduced with the inclusion of the LSH scheme. The bias and RMS error in precipitation are both improved (Table 3). This tendency to overestimate precipitation, is reflected in the general over-production of total runoff with both LSSs (Fig 4b). There is no consistent difference in the zonal mean runoff between the two LSS schemes. The positive bias in land averaged runoff increases slightly with the LSH scheme, however the RMS error is slightly reduced (Table 3). Even though the total runoff is very similar, the separate components are very different. Surface runoff dominates in the LSH scheme, whereas the CTL version produces negligible amounts over unfrozen ground (Fig 4c).

A fairer assessment of the two schemes is made by repeating the Y/P comparison. Looking at the CTL simulation of annual mean runoff to precipitation ratios, there are differences between the online (Fig 5a) and off-line (Fig 2a) studies. These are mainly the result of errors in the simulated precipitation. In particular there are more areas where Y/P is overestimated in the online study, e.g. central Africa, much of eastern Brazil. If this rainfall bias is large enough, it results in a significant overestimate of runoff and therefore Y/P. Again the new parameterisation tends to increase the runoff per unit precipitation (unless there is a significant reduction in precipitation between the CTL and LSH simulations) (Fig 5b). The RMS errors have again generally improved with the addition of the new scheme, but this is less widespread than in the off-line simulations because of the errors in rainfall. There is still an improvement in Y/P bias (from 16% to 11%) and a small reduction in the RMS error (Table 3).

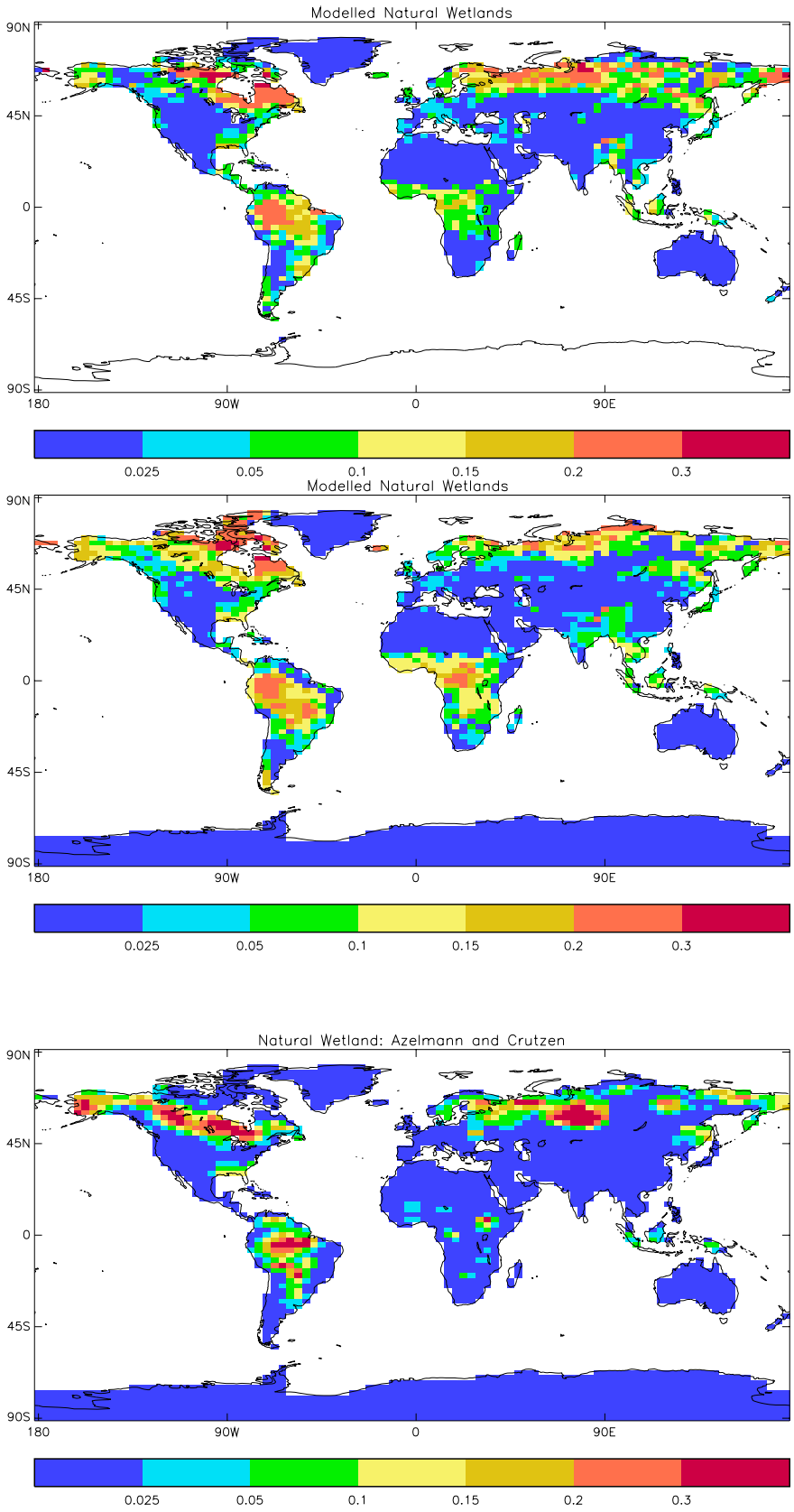

Figure 3:

The modelled natural wetland fraction compared to the observations of natural wetland area. a) and b) show the off-line and online modelled natural wetland fraction respectively. c) shows the observations of Aselmann and Crutzen (1989).

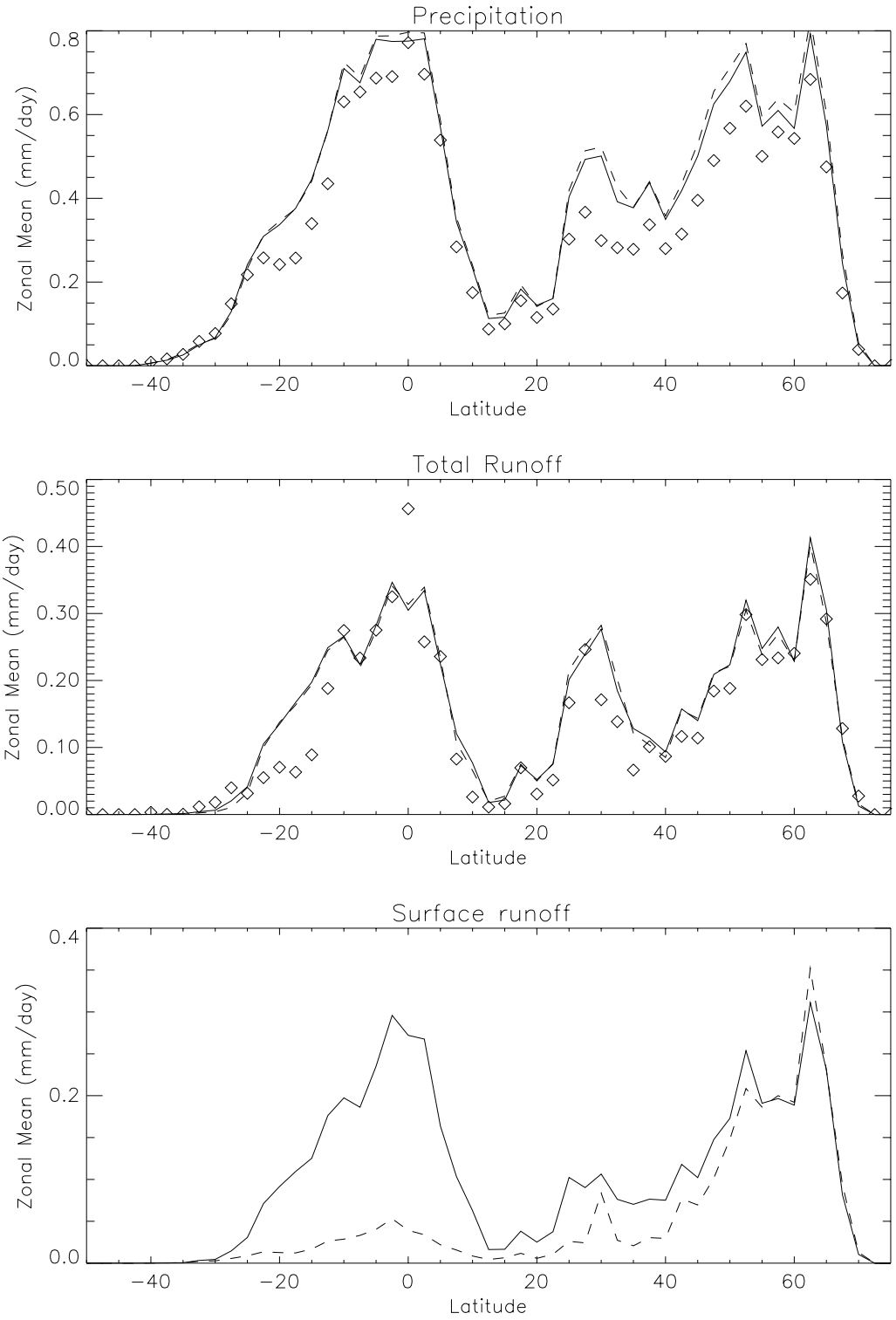

Figure 4:

1xCO2 annual average zonal mean over land simulations: a) Precipitation b) Runoff c) Surface Runoff. (Solid line (LSH), dashed line (CTL), diamonds (observations)).

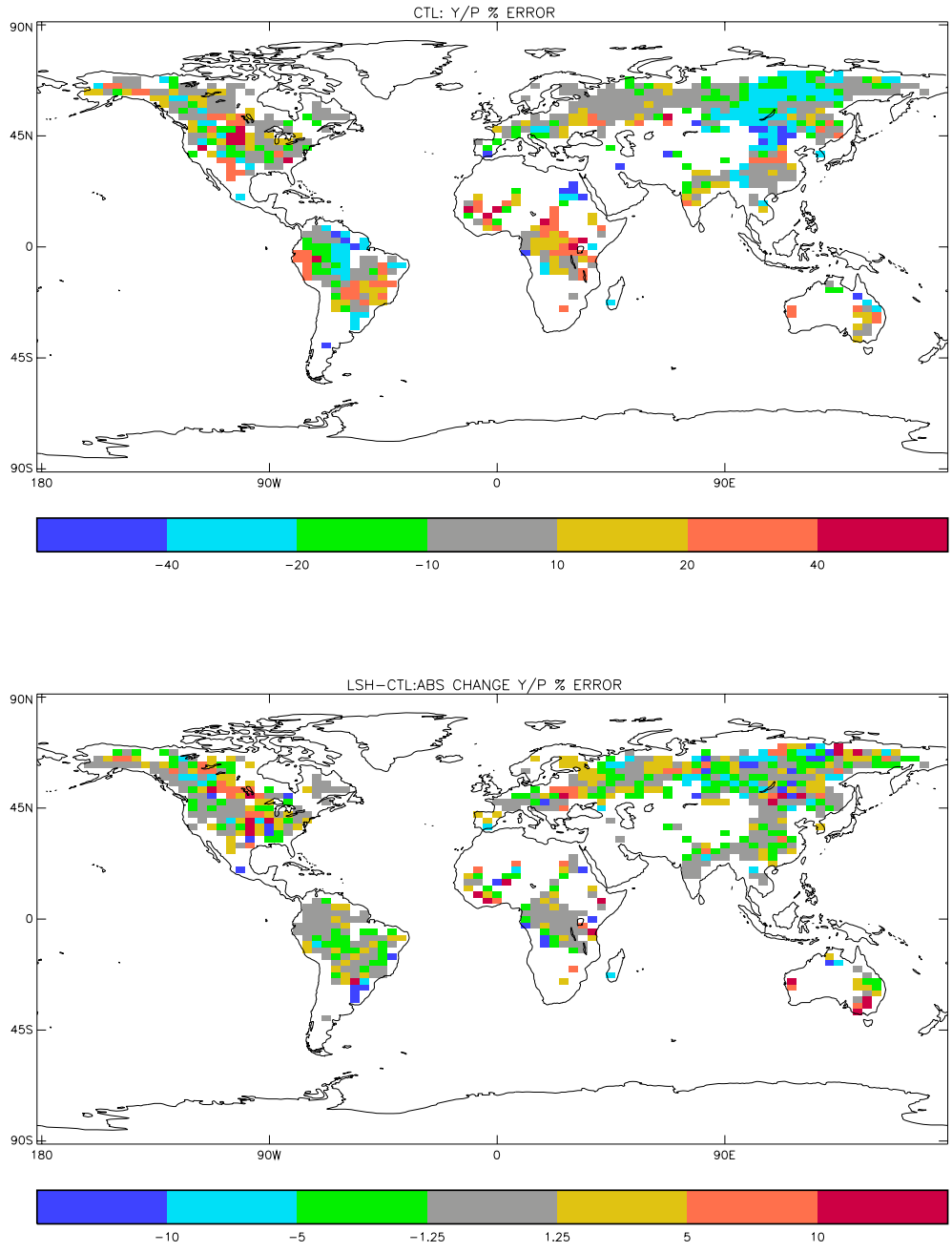

Figure 5:

As Figure 3, but for the GCM simulation.

The online estimate of natural wetland (Fig 3b) is very similar to that in the off-line study (Fig 3a). Overall the coverage seems slightly worse than the off-line simulations, indicative of errors in the GCM simulation, in particular the excessive rainfall in Central Africa.

c Climate Change

The zonal mean precipitation generally increases under the simulated climate change (Fig 6a). The main exception to this is over the southern tropics, where there is a dramatic reduction in rainfall over Amazonia (not shown). There is little difference between the predicted precipitation changes with the different LSS's. The total runoff changes (Fig 6b) tend to follow those of precipitation, again with little difference between the CTL and LSH simulations. An exception to this occurs at around 50^oN. LSH predicts a marked increase in total runoff and CTL changes little. This is because the CTL model simulates a large reduction in surface (Hortonian) runoff, due to thawing at the surface. In the LSH scheme there is still significant surface (Dunne) runoff as the water table remains relatively high at 2xCO2.

However, there are generally large differences between the surface runoff sensitivities (Fig 6c). Comparing the amplitudes of the predicted geographical changes (Figs 7a) and c)) and the zonal means (Fig 6), it is clear that much of the change in total runoff from the LSH scheme are due to surface runoff. In addition to the mid-latitude differences mentioned previously, the LSH simulation predicts increases in surface runoff over the southern tropics as the surface saturation increases. However, there is little or no change in the surface runoff in the CTL simulation outside the mid and high latitudes.

Various annual mean fields which are specific to the LSH scheme are shown in Fig 8. The tundra regions in the high latitudes and tropics are clearly depicted with very shallow water tables and extensive wetland areas in the present day simulation. Under climate change the water table depth tends to decrease (i.e. a rise in the water table) over those regions where the precipitation increases, and vice versa (see Fig 6a). The notable exception to this is over high latitude regions, especially Eurasia. Here the water table falls, in spite of the enhanced precipitation. This is because some of the frozen soil moisture melts, enhancing the drainage through the soil. Changes in the wetland area extent are a result of changes to the mean water table alone when there is no change in frozen soil water content. An increase in the water table depth reduces the surface wetland extent, and vice versa. However, over the high latitudes modifications to the seasonal freeze-thaw cycle may complicate the annual mean wetland response.

5 Conclusions

We have adapted the MOSES GCM land-surface scheme to represent the dependence of subgrid soil moisture on topography, using ideas from TOPMODEL (Beven and Kirkby (1979)). This involved introducing a mean water table within the MOSES soil model, and applying a high-resolution global dataset of the topographic index to diagnose the subgrid variation in this water table.

The revised large-scale hydrology (LSH) scheme improves the simulation of runoff in both off-line simulations (driven by observations) and online simulations (coupled to the Atmospheric GCM). In both cases the RMS error and global mean bias of annual mean total runoff are reduced. When coupled to the GCM the new model also improves the simulation of the annual mean precipitation.

The sub-gridscale distribution of water table depths can be used to estimate the saturated fraction

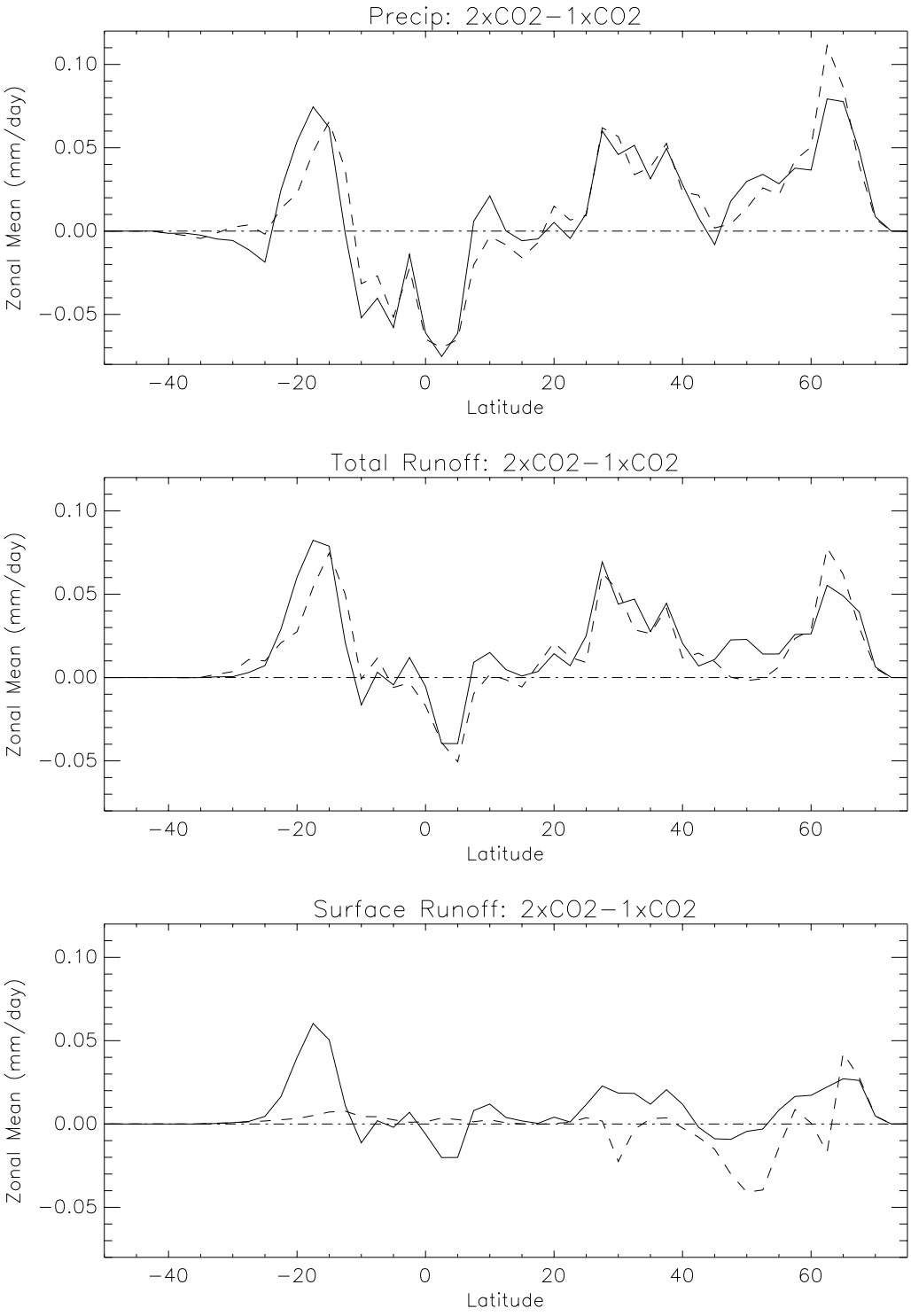

Figure 6:
2xCO2-1xCO2 annual average zonal mean over land simulations: a) Precipitation b) Runoff c) Surface Runoff. (Solid line (LSH), dashed line (CTL), diamonds (observations)).

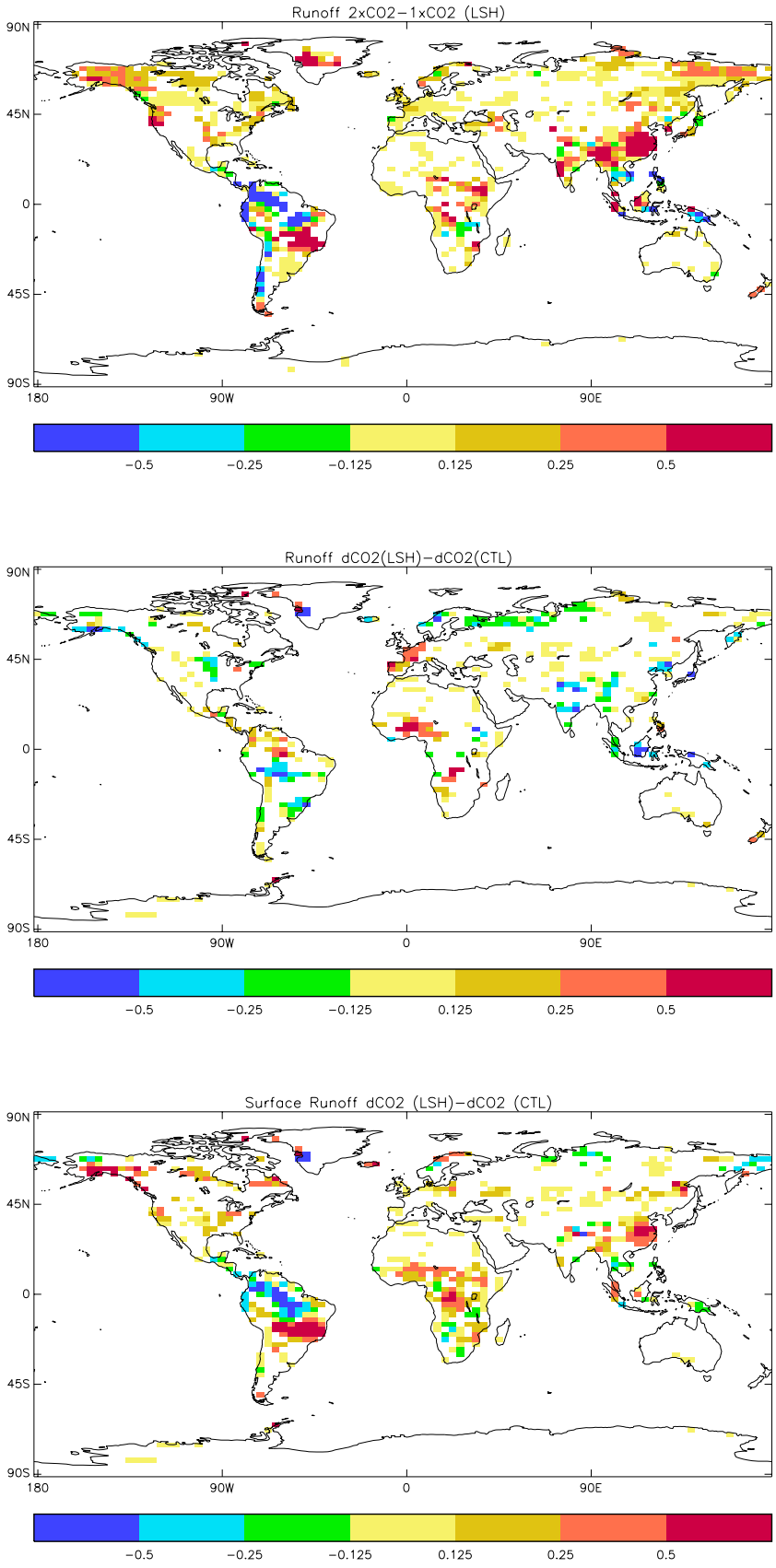

Figure 7:

Annual mean runoff sensitivity to climate change: a) 2xCO2-1xCO2 change in the total runoff for LSH. b) and c) show the difference between the sensitivity of the LSH and CTL schemes to climate change for total runoff and surface runoff respectively. (Only areas where the statistical significance is greater than 95% are shown).

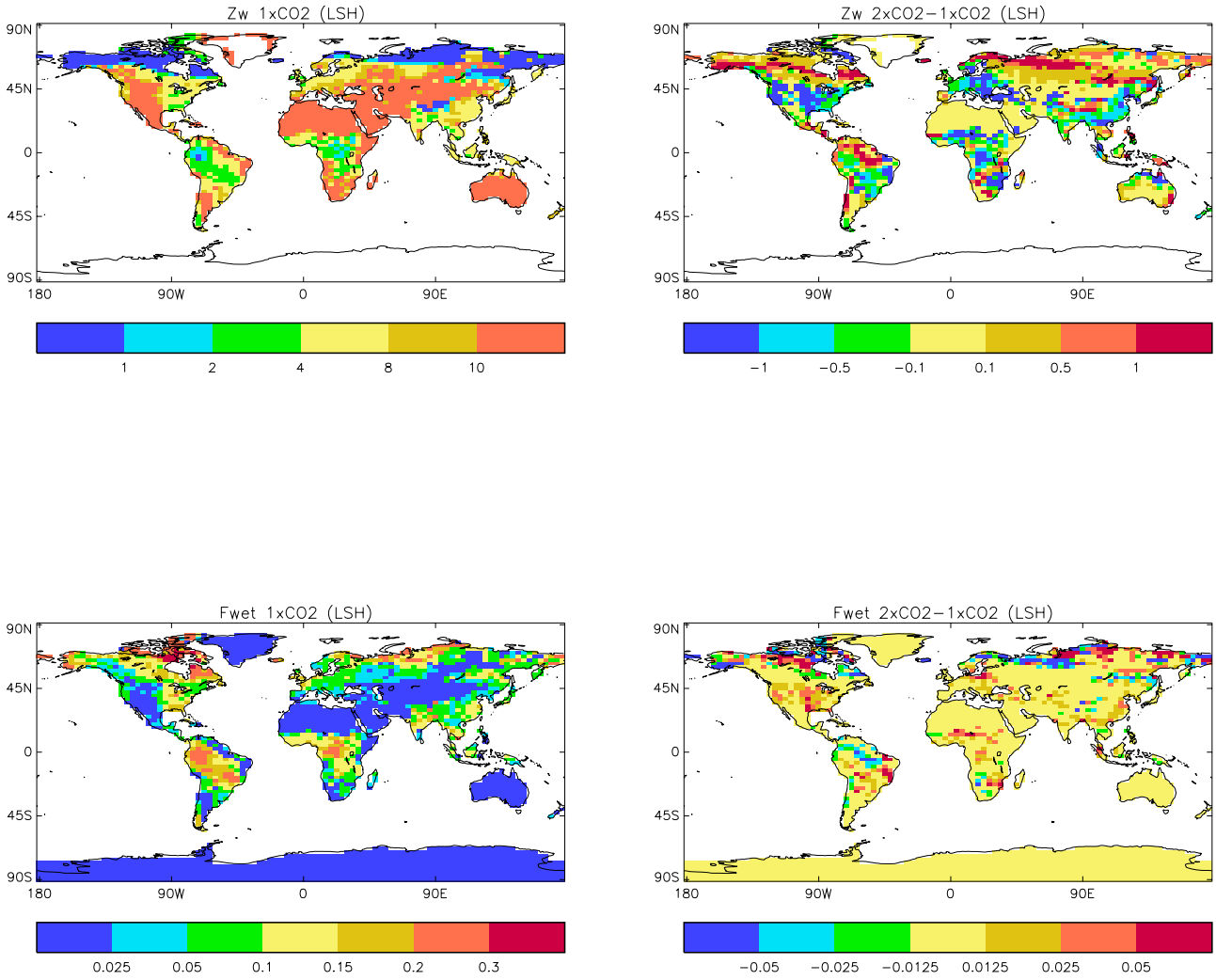

Figure 8:
1xCO2 annual mean LSH simulations and 2xCO2-1xCO2 change in the annual mean fields: a),b) Water table depth (m) c),d) Total wetland fraction.

of each gridbox, and thereby the wetland extent. This simple approach is able to reproduce most of the major wetland regions across the globe. Further improvements should be possible by including a dependence of the vertical variation of the saturated soil conductivity on soil carbon content.

The LSH scheme also influences the GCM sensitivity to doubling CO_2. Outside the mid latitudes the surface runoff is much more sensitive to climate change in the LSH scheme. Over the mid-latitudes the LSH model produces a significant increase in total runoff, whereas no such signal is evident when the standard CTL model is used. The difference can be traced to the dominant mechanisms for generating surface runoff. In the standard MOSES model surface runoff is generated mainly from frozen soils with low permeability, but in the LSH scheme the sub-gridscale soil moisture allows surface runoff generation from locally saturated soils (by the Dunne mechanism). Under climate warming many seasonally frozen soils become ice-free all year around, and this reduces mid-latitude surface runoff significantly in the standard MOSES model. Surface runoff is far less dependent on soil freezing in LSH which therefore produces less significant changes in total runoff.

The broad findings of this paper are consistent with the view that the representation of the land-surface largely determines the projected hydrological impacts under climate change (Gedney *et al* (2000)) . Improvements to the representation of subgrid soil moisture heterogeneity, such as that presented here, can be seen as a vital step towards producing useful hydrological impacts assessments online within the GCM, thereby producing internally consistent projections of climate and hydrological changes.

6 Acknowledgements

We would like to thank the UK Department for Environment, Food and Rural Affairs for support through contract PECD 7/12/37.

References

Aselmann, I., and P. Crutzen, 1989: Global distribution of natural freshwater wetlands and rice paddies, their net primary productivity, seasonality and possible methane emissions. *Journal of Atmospheric Chemistry*, **8**(4), 307–358.

Beven, K., and M. Kirkby, 1979: A physically based, variable contributing area model of basin hydrology. *Hydrological Sciences Bulletin*, **24**, 43–69.

——, 1982: On subsurface stormflow, an analysis of response times. *Hydrological Sciences Journal*, **27**, 505–521.

——, 1986: Runoff production and flood frequency in catchments of order n: an alternative approach. *Scale problems in hydrology*, et al, V. G., Ed., Kluwer, Dordrecht, Holland, 107–131.

Brown, S. R., and C. H. Scholz, 1985: Broad bandwidth study of the topography of natural rock surfaces. *J. Geophys. Res.*, **90**(B14), 2575–2582.

Cox, P. M., R. A. Betts, C. B. Bunton, R. L. H. Essery, P. R. Rowntree, and J. Smith, 1999: The impact of new land surface physics on the GCM simulation of climate and climate sensitivity. *Clim. Dyn.*, **15**, 183–203.

de Rosnay, P., J. Polcher, M. Bruen, and K. Laval, 2002: Impact of a physically based soil water flow and soil-plant interaction representation for modeling large-scale land surface processes. *J. Geophys. Res.*, **107**(D11 (art. no. 4118)).

Dirmeyer, P., A. Dolman, and N. Sato, 1999: The pilot phase of the global soil wetness project. *Bulletin of the American Meteorological Society*, **80**, 851–878.

Fekete, B. M., C. J. Vorosmarty, and W. Grabs, 2000: Global, composite runoff fields based on observed river discharge and simulated water balances. Technical report, GRDC Notes for Composite runoff fields vn1.0.

Gedney, N., P. Cox, H. Douville, J. Polcher, and P. Valdes, 2000: Characterizing GCM land-surface schemes to understand their responses to climate change. *J. Clim.*, **13**, 3066–3079.

IPCC, 2001: *Climate Change 2001: The Scientific Basis. Contribution of Working Group I to the Third Assessment Report of the Intergovernmental Panel on Climate Change*. Cambridge University Press. 881pp.

Polcher, J., P. Cox, P. Dirmeyer, H. Dolman, H. Gupta, A. Henderson-Sellers, P. Houser, R. Koster, T. Oki, A. Pitman, and P. Viterbo, 2002: Glass : Global land-atmosphere system study. *GEWEX News*, **5**.

Pope, V. D., M. L. Gallani, P. R. Rowntree, and R. A. Stratton, 2000: The impact of new physical parametrizations in the Hadley Centre climate model – HadAM3. *Climate Dyn.*, **16**, 123–146.

Sivapalan, M., K. Beven, and E. Wood, 1987: On hydrological similarity. 2. a scaled model of storm runoff production. *Water Resources Research*, **23**, 2266–2278.

UNESCO, 1971: Discharge of selected rivers of the world. Studies and reports in hydrology 5, UNESCO.

Verdin, K. L., and S. K. Greenlee, 1996: Development of continental scale digital elevation models and extraction of hydrographic features. *Proceedings, Third International Conference/Workshop on Integrating GIS and Environmental Modeling.* National Center for Geographic Information and Analysis, Santa Barbara, California.

Xie, P., and P. A. Arkin, 1997: Global precipitation: A 17-year monthly analysis based on gauge observations, satellite estimates and numerical model outputs. *Bull. Am. Meteorol. Soc.*, **78**(11), 2539–2558.